

# Pico Lantern: A Pick-up Projector for Augmented Reality in Laparoscopic Surgery

Philip Edgcumbe<sup>1</sup>, Philip Pratt<sup>2</sup>, Guang-Zhong Yang<sup>2</sup>,  
Chris Nguan<sup>3</sup>, and Rob Rohling<sup>1,4</sup>

<sup>1</sup>Department of Electrical and Computer Engineering,  
University of British Columbia, Vancouver, BC, Canada  
{edgcumbe, rohling}@ece.ubc.ca

<sup>2</sup>Hamlyn Centre for Robotic Surgery  
Imperial College of Science, Technology and Medicine, London, UK  
{p.pratt, g.z.yang}@imperial.ac.uk

<sup>3</sup>Department of Urologic Sciences  
University of British Columbia, Vancouver, BC, Canada  
chris.nguan@ubcurology.com

<sup>4</sup>Mechanical Engineering, University of British Columbia, Vancouver, BC, Canada

**Abstract.** The Pico Lantern is proposed as a new tool for guidance in laparoscopic surgery. Its miniaturized design allows it to be picked up by a laparoscopic tool during surgery and tracked directly by the endoscope. By using laser projection, different patterns and annotations can be projected onto the tissue surface. The first explored application is surface reconstruction. The absolute error for surface reconstruction using stereo endoscopy and untracked Pico Lantern for a plane, cylinder and *ex vivo* kidney is 2.0 mm, 3.0 mm and 5.6 mm respectively. The absolute error using a mono endoscope and a tracked Pico Lantern for the same plane, cylinder and kidney is 0.8mm, 0.3mm and 1.5mm respectively. The results show the benefit of the wider baseline produced by tracking the Pico Lantern. Pulsatile motion of a human carotid artery is also detected *in vivo*. Future work will be done on the integration into standard and robot-assisted laparoscopic surgery.

**Keywords:** pico projector, laparoscopic surgery, augmented reality.

## 1 Introduction

Laparoscopic surgery is minimally invasive and has several advantages over open surgery. However, one disadvantage is the reduced visibility through the endoscope. In particular, monocular endoscopy reduces the ability to perceive the depth of the tissue surface and spatial relationships. Several companies market stereo endoscopy cameras as a way to improve visual perception, but they are not widely used. Two examples are the Viking 3DHD Vision System (Viking Systems, Westborough, MA, USA) and the Endoeye Flex 3D (Olympus, Shinjuku, Tokyo, Japan).

The da Vinci robotic system for minimally invasive surgery (Intuitive Surgical, Sunnyvale, CA) offers stereo vision and dexterous tele-manipulation of the surgical tools and camera. Because of these advantages it has become the predominant system

for several types of surgery in the United States, such as radical prostatectomy (RP). RP is a common treatment for prostate cancer, the second leading cause of cancer-related deaths for men in the United States. During RPs, preservation of the neurovascular bundle near the prostate helps maintain potency and continence. In this and other applications, there is a clear need for accurate guidance tools in both standard and robotic surgery to see subsurface anatomy such as blood vessels and nerves.

There is a wealth of research on a wide range of guidance tools for minimally invasive surgery. One research area is augmented reality (AR). An early example of AR in laparoscopic surgery used a combination of a camera, projector and helmet-mounted display of computer-generated subsurface anatomy structures [1]. Ongoing challenges include the accurate registration and alignment of the structures with the possibly deformed tissue [2, 3], the transformation of the structures into the endoscope view, and the natural depiction and spatial perception of structures [4].

A common requirement in many surgical guidance tools is the ability to reconstruct the 3D surface of the tissue accurately and quickly. A recent survey paper on this topic [5] provides a highly detailed review of the state of the art. The five main approaches are stereo endoscopy (requiring a stereo endoscope), monocular shape-from-X, SLAM (Simultaneous Localization and Mapping from a moving camera), time-of-flight from a specialized illumination unit, and structured light. All methods have advantages and disadvantages. We are particularly interested in structured light because of its advantages in speed, accuracy, and ability to map even smooth featureless organ surfaces. One approach is a sophisticated multi-spectral fiber-based structured light probe [6]. It has a diameter of 1.7 mm and it can fit in the biopsy channel of an endoscope. It projects 127 differently colored spots which are uniquely identified in the endoscope images. The spot colors are fixed so it cannot project AR.

This paper describes a new low cost (<\$500US) source of structured light and AR that leverages recent advances in laser-based pico projectors. It uses the laser diodes and a micro electro mechanical system (MEMS) from the Microvision ShowWX+ projector (Redmond, WA, USA). The proposed system is called a “Pico Lantern” because it is designed to be dropped into the abdominal cavity, then picked up and moved around the cavity to illuminate a region of interest. We have three Pico Lantern prototypes with nearly identical hardware components. The first is the calibrated ShowWX+ projector used for the experiments in this paper. The second separates the integrated photonics module (IPM) and electronics platform module (EPM) of the ShowWX+ projector via a new housing and cabling so that the EPM is kept outside of the patient (Fig. 1). It has the same 3-color functionality as the ShowWX+ projector, a diameter of 28 mm and it can be placed through the skin incision with the cable beside the trocar. It has the same grasp as in Schneider *et al.* [7] so it is compatible with the da Vinci robot. The third prototype (Fig. 1) has a diameter of 12mm and it can be placed through a trocar. In the third prototype two of the three laser diodes have been removed and the one blue laser is in a new location. This prototype is still under development.

As mentioned above, the use of projectors in surgery has a long history [1]. What is new here is leveraging the miniaturization of projectors for consumer electronics to create a pick-up projector for laparoscopic surgery. The Pico Lantern image is always in focus because it has a raster scanning laser pico projector (MEMS scanner mirror: 2.9×2.2×1 mm) and a single-pixel beam expansion that matches the rate of expansion

of the projected image size. It can project on any surface, including irregular surfaces, with a higher sharpness, contrast, and color space than non-laser projectors [8].

The Pico Lantern can project different patterns and annotations from a range of positions in the cavity. Thus, augmented reality can be implemented by directly projecting computer-generated structures on the tissue surface using the same coordinate system transformations used to calculate the 3D tissue surface. There are challenges of projecting on curved non-white surfaces, but solutions to these problems have been proposed [9]. It is possible to modify the projected pattern on the curved surface so that it appears undistorted in the endoscope view [10]. Like a real lantern, several other uses for the Pico Lantern could be envisioned in addition to the delivery of structured light. For example, the Pico Lantern could be simply used as a supplementary light source that can cast shadows of small surface features when lit from a shallow angle. It could also reduce undesired bright specular reflections from a constant light source by reducing the illumination of only those reflecting regions (seen in the camera and converted to Pico Lantern coordinates). The da Vinci surgical system is ideal for testing the Pico Lantern because it can hold the Pico Lantern steady in different poses. It also has a stereo endoscope to help reconstruct the 3D tissue surface.

In summary, tests on phantoms and animal tissue demonstrate the feasibility and accuracy of 3D tissue surface reconstruction using the Pico Lantern with a stereo endoscope and mono endoscope. Novel aspects include the explicit tracking of the Pico Lantern, the detection with the Pico Lantern of tiny tissue movement from the pulsatile motion of an underlying blood vessel and showing how the image projected by the Pico Lantern for AR could enhance the appearance of that motion.

## 2 Methods and Materials

### 2.1 Materials

A 1280×960 pixel Flea2 camera (Point Grey Research, Richmond, Canada) is used for the laser calibration. All tests are done using a da Vinci Si Surgical System with images of 1280×1024 pixels. The Pico Lantern has an HDMI input, a frame rate of 60 Hz, projection resolution of 848×480 pixels, and a brightness of 15 lumens.

A checkerboard with 3.175 mm squares is affixed onto a flat surface of the Pico Lantern prototypes. The inner 2x6 checks and associated saddle points (suitable for the 12mm prototype) are used for tracking. The checkerboard is made of surgical identification tape (Key Surgical Inc., MN, USA) that is designed to be semi-permanently attached to surgical instruments through repeated sterilization cycles, and it is approved for use in humans [11].

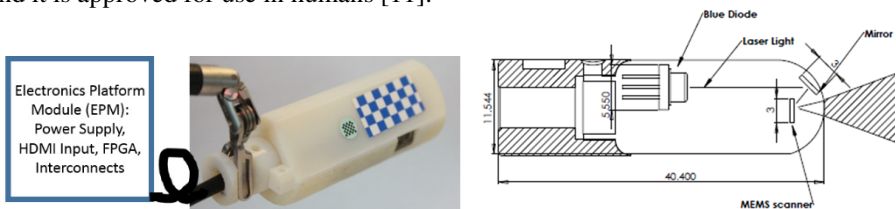


**Fig. 1.** Picture of Pico Lantern prototype #2 with tether to external electronics platform module (left), and schematic of the Pico Lantern prototype # 3 with units of mm (right)

## 2.2 3D Surface Reconstruction

Two methods are proposed for 3D surface reconstruction in the two sections below:

### 2.2.1 Method 1 - Stereo Endoscope and Untracked Pico Lantern

In method 1, the Pico Lantern projects a checkerboard pattern onto the surface for stereo-correspondence determination between left and right cameras to calculate the 3D position of the checkerboard saddle points [12].

### 2.2.2 Method 2 - Mono endoscope and Tracked Pico Lantern

Method 2 is suitable for either a mono or stereo endoscope; mono vision is used here. The location of the Pico Lantern, in the coordinate system of the endoscope/camera, is determined by visually tracking the checkerboard that is affixed to the Pico Lantern. This enables surface reconstruction using *wide baseline* triangulation with the camera and Pico Lantern at two of the vertices of the triangle. The 3D position of each projected checkerboard saddle point is at the third vertex of the triangle and is at the intersection of the ray  $V$  (from P to a saddle point in I, converted using  ${}^I T_P$ ) of the Pico Lantern and the corresponding ray  $R$  (from C to saddle point in I, converted using  ${}^I T_C$ ) in the camera images (Eqn. 1) [12].

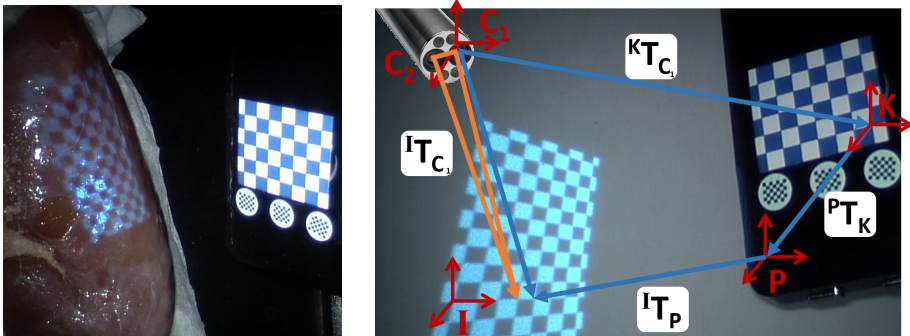


**Fig. 2.** Projection of blue checkerboard onto an *ex vivo* kidney with medium intensity lighting (40/100) from the da Vinci Si light source (left). Overview of the two methods used for surface reconstruction (right). The orange lines show the narrow-triangle geometry of method 1 and the blue lines show the wider geometry of method 2.

The Caltech Camera Calibration stereo triangulation toolbox [13] is used to solve the scalar parameters  $s$  and  $u$  to determine the coordinates of the saddle points on the object. §

$${}^C \begin{bmatrix} sR_x & sR_y & sR_z & s \end{bmatrix} = {}^C T_P * {}^P \begin{bmatrix} uV_x & uV_y & uV_z & u \end{bmatrix} \quad (1)$$

The transformation from the projector to camera coordinate system,  ${}^C T_P$ , is equal to  ${}^C T_K * {}^K T_P$  where  ${}^C T_K$  is the transformation from the Key Surgical checkerboard (K) on the Pico Lantern to the camera (C) that is calculated in each camera frame (C), and  ${}^K T_P$  is the fixed transformation from the Pico Lantern keyhole aperture (P) to the Key Surgical checkerboard (K).  ${}^K T_P$  is calibrated offline using corresponding points

between the known location of projected checkerboard saddle points onto a plane in the Pico Lantern (P) and Key Surgical checkerboard (K) coordinates [14]. Twelve images from the Flea2 camera with 98 points each are used for this calibration. The method uses the Bouguet's Camera Calibration Toolbox [13] which is based on Zhang's algorithm [15]. The key is to model the projector as a camera in reverse. The endoscope cameras are also calibrated for intrinsic and extrinsic parameters [13].

### 2.2.3 Saddle Point Selection

For method 1 and method 2, regions with saddle points are selected manually, and the saddle point detection algorithm [13] is then used to determine the checkerboard corner locations with sub-pixel accuracy. In the future, an automatic tracking algorithm will be implemented that has been successfully used on porcine [16] and human [17] surgical subjects, hence the extra circular targets in Fig. 2.

## 2.3 Validation of 3D Surface Reconstruction

The objects for 3D surface reconstruction are a white plane, cylinder ( $52.63 \pm 0.05$  mm diameter) and an *ex vivo* porcine kidney for a more realistic appearance of a tissue surface. For each object, the camera and object remained in the same position and the Pico Lantern is moved to 5 different poses within the field of view of the stationary endoscope. The surface data from the 5 poses are then combined together. The identical images and poses are used for evaluating the accuracy of both 3D surface reconstruction methods. For all the surface reconstruction tests, the average and standard deviation of the distance from camera to object, distance from Pico Lantern to object, and angle between the Pico Lantern and camera axes is  $166 \pm 7$  mm,  $49 \pm 11$  mm and  $61^\circ \pm 12^\circ$  respectively. The da Vinci Si endoscope surgical light is set to a medium brightness (40/100) as a compromise between ambient lighting and projected contrast.

For all tests, a Certus optical tracker (NDI, Waterloo, Canada) stylus measured the plane, cylinder and kidney surfaces. The *relative error* is the average distance from the fitted plane and cylinder shape to the Pico Lantern measured surface points. The *absolute error* is the average distance from the Certus measured surfaces of the plane/cylinder/kidney to the Pico Lantern measured surface points. To minimize tissue deformation from the stylus, the kidney is frozen and only the surface is defrosted.

## 2.4 Augmented Reality Display of Tissue Movement

The Pico Lantern can be used to both *measure* pulsatile motion of a subsurface artery using the above method, and *depict* its motion/location. There are challenges for depicting computer-generated features such as vessels, and suitable visual cues have been proposed by others [4]. Here we propose to simply display dots that are sized in proportion to the surface motion in the frequency domain of 0.82–1.1 Hz over a 10 second period. By combining the checkerboard and dots, measurement and depiction can be simultaneous. The projector and endoscope is pointed towards the carotid artery of the volunteer, and method 2 is used to track the 3D surface map of the region.

### 3 Results

The 3D surface reconstruction relative error for method 1 was  $1.6 \pm 1.6$  mm for the plane and  $2.4 \pm 2.1$  mm for the cylinder. The relative error for method 2 was  $0.8 \pm 0.7$  mm for the plane, and  $0.3 \pm 0.3$  mm for the cylinder. The absolute error for method 1 was  $2.0 \pm 1.7$  mm for the plane,  $3.0 \pm 2.9$  mm for the cylinder and  $5.6 \pm 4.9$  mm for the kidney. The absolute error for method 2 was  $1.4 \pm 1.1$  mm for the plane,  $1.5 \pm 0.6$  mm for the cylinder and  $1.5 \pm 0.6$  mm for the kidney. During data collection, the range of covered by the Pico Lantern, in the camera coordinate system, was  $27 \times 21 \times 49$  mm for the plane,  $14 \times 53 \times 36$  mm for the cylinder and  $20 \times 28 \times 29$  mm for the kidney. The extent of the *ex vivo* kidney surface included in the surface reconstruction is shown in Fig. 3.

The results of the *in vivo* human test of the pulsatile motion of the neck near the carotid artery is shown in the right of Fig. 3. The dot size corresponds to the magnitude of the pulsatile motion in the frequency range of 0.82–1.1 Hz. The larger dots denotes the carotid artery path that runs vertically through the image on the right side of the checkerboard. The carotid artery path was determined by typical anatomical landmarks and the pulsation sensed by palpation. The top graph in Fig. 3 shows the periodic pulsatile displacement of a saddle point which has a maximum 3D vector magnitude of 0.9mm. The lower graph shows a point that is about 10mm away from the carotid artery and has a maximum displacement of 0.3mm and is not as periodic.

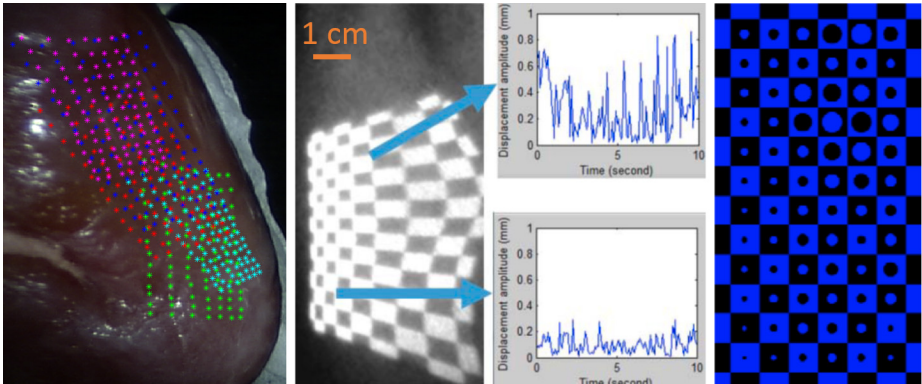


**Fig. 3.** Endoscope view of the combined surface measurements of the *ex vivo* kidney with the Pico Lantern projector in five different locations (left). Endoscope view while measuring motion of the human neck *in vivo* with graphs showing 10 secs of displacement of the saddle points indicated by the arrows (middle). Depiction of the motion of the carotid artery using dot size: large dots correspond to large motion (right).

### 4 Discussion and Conclusion

In this paper we have proposed the Pico Lantern, a pick-up laser projector for minimally invasive surgical guidance that is based on low-cost, fast, commercially available technology. We test the surface reconstruction accuracy that can be achieved using the Pico Lantern and show it can stitch multiple views of the surface

together. Method 1 uses a stereo endoscope with an untracked Pico Lantern method and achieves an accuracy comparable to other stereo endoscope results for the plane and cylinder [18]. However, it is sensitive to the detection of the saddle point, so the accuracy decreases for the kidney because a simple correspondence method is used, the surface of the kidney causes the projected image to become blurrier and the stereo endoscope has a small baseline of 5mm. Method 2, the mono endoscope with tracked Pico Lantern, was more accurate and consistent. This is because method 2 has a wide baseline between the camera/endoscope and Pico Lantern and the high-contrast checkerboard on the Pico Lantern make it easy to accurately track. Other potential advantages of method 2 include: easier identification of the structured light features in the endoscope view since the Pico Lantern rays can be calculated in camera coordinates; mono-vision endoscopy to be used in 3D surface reconstruction; particular effectiveness compared to other technique on tissues with a low density of natural and unique surface features; it can cover a wide region of interest by stitching reconstructed surfaces together; the surgeon can move the Pico Lantern as close as necessary to achieve desired accuracy/field-of-view tradeoff; an effective way to add AR which only requires the laparoscopic video feed and does not require any change to the laparoscopic hardware. The sub-millimeter level relative accuracy of the method 2 mono endoscope approach compares very favorably to surface reconstruction techniques in which a single mono endoscope is used with no additional components. As mentioned previously, Clancy *et al.* used a mono-endoscope and multi-spectral illumination and reported sub-millimeter relative accuracy for fitting a plane and cylinder, but they kept their structured light source in a fixed position relative to the camera throughout the experiment and did not report the baseline distance between the structured light source and mono endoscope [6].

A disadvantage of method 2 is that the Pico Lantern must be in the field of view of the endoscope. More general disadvantages of the Pico Lantern are: the need to grasp and manipulate the Pico Lantern (the da Vinci 3<sup>rd</sup> arm may be a solution); a tether through an additional port (or the tether could be squeezed between an existing trocar and tissue, as suggested for the pick-up ultrasound transducer [7]); the brightness is limited (this is the same for consumer electronics and luminance continues to improve); the Pico Lantern requires additional hardware, unlike stereo endoscopy.

As pico projector technology continues to improve, we will see further improvements in accuracy, luminance, resolution, miniaturization and cost. In conclusion, a proof-of-concept of the Pico Lantern suggests sub-millimeter surface reconstruction is possible and could be used for detecting and displaying subsurface pulsatile vessel motion. The next steps include sterilization and clinical validation.

**Acknowledgements.** This work was funded by CIHR and NSERC and proudly funded by Prostate Cancer Canada – Grant # GS2014-05. Thanks to Caitlin Schneider and Tim Salcudean for advice, help and equipment.

## References

1. Fuchs, H., et al.: Augmented Reality Visualization for Laparoscopic Surgery. In: Wells, W.M., Colchester, A.C.F., Delp, S.L. (eds.) MICCAI 1998. LNCS, vol. 1496, pp. 934–943. Springer, Heidelberg (1998)

2. Pratt, P., Stoyanov, D., Visentini-Scarzanella, M., Yang, G.-Z.: Dynamic Guidance for Robotic Surgery Using Image-Constrained Biomechanical Models. In: Jiang, T., Navab, N., Pluim, J.P.W., Viergever, M.A. (eds.) MICCAI 2010, Part I. LNCS, vol. 6361, pp. 77–85. Springer, Heidelberg (2010)
3. Benincasa, A.B., Clements, L.W., Duke Herrell, S., Galloway, R.L.: Feasibility study for image-guided kidney surgery: Assessment of required intraoperative surface for accurate physical to image space registrations. *Med. Phys.* 35(9), 4251–4261 (2008)
4. Hansen, C., Wieferich, J., Ritter, F., Rieder, C., Peitgen, H.-O.: Illustrative Visualization of 3D Planning Models for Augmented Reality in Liver Surgery. *IJCARS* 5, 133–141 (2010)
5. Maier-Hein, L., Mountney, P., Bartoli, A., Elhawary, H., Elson, D., Groch, A., Kolb, A., Rodrigues, M., Sorger, J., Speidel, S., Stoyanov, D.: Optical Techniques for 3D Surface Reconstruction in Computer-Assisted Laparoscopic Surgery. *Med. Img.* 17, 974–996 (2013)
6. Clancy, N.T., Stoyanov, D., Maier-Hein, L., Groch, A., Yang, G.-Z., Elson, D.S.: Spectrally Encoded Fiber-Based Structured Lighting Probe for Intraoperative 3D Imaging. *Biomedical Optics Express* 2(11), 3119–3128 (2011)
7. Schneider, C., Guerrero, J., Nguan, C., Rohling, R., Salcudean, S.: Intra-operative “Pick-Up” Ultrasound for Robot Assisted Surgery with Vessel Extraction and Registration: A Feasibility Study. In: Taylor, R.H., Yang, G.-Z. (eds.) IPCAI 2011. LNCS, vol. 6689, pp. 122–132. Springer, Heidelberg (2011)
8. Lincoln, J.: March of the Pico Projectors. *IEEE Spectrum* 47, 40–45 (2010)
9. Park, H., Lee, M.-H., Kim, S.-J., Park, J.-I.: Surface-Independent Direct-Projected Augmented Reality. In: Narayanan, P.J., Nayar, S.K., Shum, H.-Y. (eds.) ACCV 2006. LNCS, vol. 3852, pp. 892–901. Springer, Heidelberg (2006)
10. Tardif, J.P., Roy, S., Meunier, J.: IEEE: Projector-based augmented reality in surgery without calibration. In: *IEEE EMBS*, pp. 548–551. IEEE Press, New York (2003)
11. Edgcumbe, P., Nguan, C., Rohling, R.: Calibration and Stereo Tracking of a Laparoscopic Ultrasound Transducer for Augmented Reality in Surgery. In: Liao, H., Linte, C.A., Masamune, K., Peters, T.M., Zheng, G. (eds.) MIAR 2013 and AE-CAI 2013. LNCS, vol. 8090, pp. 258–267. Springer, Heidelberg (2013)
12. Geng, J.: Structured-Light 3D Surface Imaging: a Tutorial. *Advances in Optics and Photonics* 3, 128–160 (2011)
13. Bouguet, J.-Y.: Visual Methods for Three-dimensional Modeling, Phd Thesis (1999)
14. Falcao, G., Hurtos, N., Massich, J., Fofi, D.: Projector-Camera Calibration Toolbox. *Erasmus Mundus Masters in Vision and Robotics* (2009)
15. Zhang, Z.: A Flexible New Technique for Camera Calibration. *IEEE T PAMI* 22, 1330–1334 (2000)
16. Pratt, P., Di Marco, A., Payne, C., Darzi, A., Yang, G.-Z.: Intraoperative ultrasound guidance for transanal endoscopic microsurgery. In: Ayache, N., Delingette, H., Golland, P., Mori, K. (eds.) MICCAI 2012, Part I. LNCS, vol. 7510, pp. 463–470. Springer, Heidelberg (2012)
17. Hughes-Hallett, A., Pratt, P., Mayer, E., Di Marco, A., Yang, G.-Z., Vale, J., Darzi, A.: Intraoperative Ultrasound Overlay in Robot-assisted Partial Nephrectomy: First Clinical Experience. *Eur. Urol.* 65(3), 671–672 (2014)
18. Röhl, S., Bodenstedt, S., Suwelack, S., Dillmann, R., Speidel, S., Kenngott, H., Müller-Stich, B.P.: Dense GPU-Enhanced Surface Reconstruction From Stereo Endoscopic Images for Intraoperative Registration. *Med. Phys.* 39, 1632–1645 (2012)